R&D NOTE

Buildup of High Solids Flux Conveying Flow by Coupling a Moving Bed to the Riser Bottom

Xinhua Liu
State Key Laboratory of Multi-Phase Complex System, Institute of Process Engineering, Chinese Academy of Sciences, Beijing 100190, China

Xin Cui
School of Chemical Engineering, Shenyang Institute of Chemical Technology, Shenyang 110142, China

Guang Sun
Faculty of Chemical Engineering, China University of Petroleum, Beijing 102249, China

Toshiyuki Suda and Masahiro Narukawa
Research Laboratory, IHI Corporation Ltd. (IHI), Isogo-Ku, Yokohama 235-8501, Japan

Yunyi Liu
School of Chemical Engineering, Shenyang Institute of Chemical Technology, Shenyang 110142, China

Guogang Sun
Faculty of Chemical Engineering, China University of Petroleum (Beijing), Beijing 102249, China

Guangwen Xu
State Key Laboratory of Multi-Phase Complex System, Institute of Process Engineering, Chinese Academy of Sciences, Beijing 100190, China

DOI 10.1002/aic.11861
Published online July 13, 2009 in Wiley InterScience (www.interscience.wiley.com).

Keywords: high solids flux, circulating fluidized bed, dual fluidized bed, transport bed, gasification

Introduction

Circulating fluidized bed (CFB) technology was first developed for the fluid catalytic cracking of crude oil in the 1940s, which is mainly characterized by circulating the solids between two adjacent fluidized vessels. Based on the CFB technology, dual fluidized bed gasification (DFBG) was proposed in the 1980s, but it received renewed interest in recent years as a high efficiency solids fuel gasification process for the production of high-quality syngas.[1] In an autothermal DFBG system, heat transfer from the exothermal fluidized bed combustor to the endothermal fluidized bed pyrolyzer/gasifier, especially for pure steam gasification, relies on rapid and large solids circulation between the two vessels. A higher solids circulation rate, G_s, allows small temperature difference between the two reactors, thus making the operation and control of the DFBG system much easier. Transport bed gasification (TBG) is another newly developed thermochemical conversion method based on the CFB technology.[2] The TBG process has the advantages of low tar evolution, modest reaction temperature, and high

Correspondence concerning this article should be addressed to G. Xu at gwxu@home.ipe.ac.cn

© 2009 American Institute of Chemical Engineers

fuel adaptability and throughputs. The implementation of these merits, however, is premised by excellent gas–solids and solids–solids contact in the transport bed gasifier, thereby also requiring high solids circulation rates in the TBG system.

When a riser operates in the fast fluidization and dense suspension upward flow regime, the solids circulation rate (G_s) is mainly determined by the pressure balance between the riser and the returning loop.[3] In this case, the maximal G_s achievable in the riser can be increased by minimizing the pressure loss across the solids feed control valve or maximizing the pressure head from the returning loop. Adopting a screw feeder instead of the nonmechanical seal valve in the CFB system seems to be an efficient way to increase the G_s, but it is not suitable for scaling up of high-temperature processes such as the DFBG and TBG systems. Pugsley et al.[4] developed a novel nonmechanical solids feeder to realize high solids fluxes in the riser, whereas their design involved replacing the traditional standpipe and L-valve with the complex combination of an aerated annular bed and a radial gas distributor for the riser. Coupling a secondary riser with a large cross-sectional area[3] or another downer-riser system[5] to the CFB riser was reported to be feasible to increase the solids flux in the first riser; however, both the methods dramatically increase the complexity of the whole system.

In a traditional CFB shown in Figure 1a, the largest pressure drop, ΔP_{tra}, realizable in the returning loop can be estimated as follows:

$$\Delta P_{tra} = \Delta P_{s,tra} - \Delta P_{loop} = (\Delta P_I + \Delta P_{II}) - \Delta P_{loop}. \quad (1)$$

Because the unavoidable flow resistance ΔP_{loop} of the loop seal at the bottom partially counteracts the pressure head $\Delta P_{s,tra}$ induced by the particle bed in the standpipe and makes it impossible to be completely converted into the effective feed driving force, the G_s in the traditional CFB is hardly greater than about 200 kg/(m^2·s).[6] Taking this into consideration, the authors proposed an idea of coupling a moving bed to the riser bottom to elevate the feed driving force of the returning loop and thereby to increase the solids flux in the riser. In this new design, a throat-type configuration instead of the loop seal, as denoted by the short dashed lines in Figure 1b, was adopted at the bottom of the moving bed to allow both the accumulation of recycling particles inside the bed and the introduction of fluidizing gas into the bed. The loop seal was leveled up above the moving bed to prevent the backflow of the gas from the moving bed to the standpipe. The loop seal fluidizing air (U_{gu}) and the moving bed aeration air (U_{gm}) can be introduced into either the bottom section of the riser as marked by the long dashed lines in Figure 1b or the downstream line as the product gas in the actual DFBG system. As shown in Figure 1b, the greatest pressure drop ΔP_{new} achievable in the returning loop of the new CFB reconfigured according to the aforementioned idea can be expressed as follows:

$$\Delta P_{new} = (\Delta P_{s,new} - \Delta P_{loop}) + (\Delta P_m - \Delta P_{throat}) = (\Delta P_I - \Delta P_{loop}) + (\Delta P_m - \Delta P_{throat}). \quad (2)$$

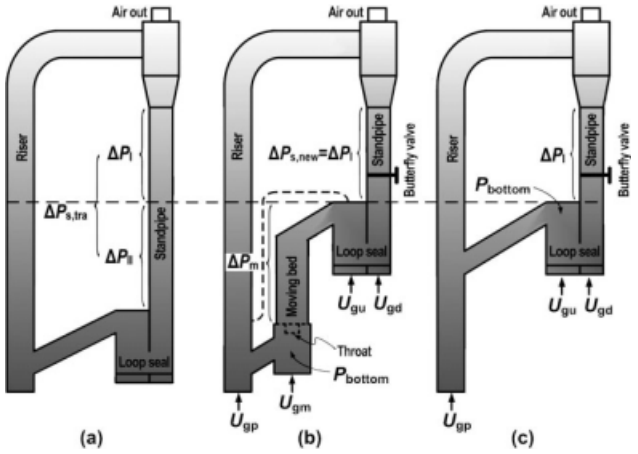

Figure 1. Principle of the proposed idea and different bed configurations.

(a) Traditional CFB; (b) newly configured CFB/simulated traditional CFB I; (c) simulated traditional CFB II.

Thus, a possible much greater pressure head ΔP_m from the moving bed in the newly configured CFB than the ΔP_{II} from the bottom section of the standpipe in the traditional CFB may be directly exerted on the gas–solids flow inside the riser, because the extra flow resistance ΔP_{throat} induced by the throat-type exit of the moving bed is expected to be rather small. Therefore, the largest effective feed driving force ΔP_{new} available in the returning loop of the newly configured CFB may be much greater than the ΔP_{tra} in the traditional CFB.

This short communication aims to discuss the buildup of high solids fluxes in the new CFB reconfigured according to the aforementioned novel idea. Comparing the experimental data from the newly configured CFB with those from two simulated traditional CFBs as well as the calculation results from a well-known correlation, the preceding idea and the involved flow mechanism will be clarified further.

Experimental and Results

Figure 1b shows a sketch of the laboratory-scale CFB reconfigured according to the above proposed idea. The newly configured CFB is made of Plexiglas and mainly consists of a 12.4 m high, 90 mm i.d. riser, a 7.4 m high, 80 mm i.d. standpipe, a 0.35 m × 0.20 m × 0.60 m cuboid-shaped loop seal, and a 4.4 m high, 120 mm i.d. moving bed. To simulate the traditional CFB, the throat-type configuration was removed in comparative tests to enable the recycling particles to flow through the column rapidly. Under this condition, the column was used only as a part of a common standpipe and the modified CFB was actually operated in a simulated traditional CFB mode. This modified bed configuration will be denoted as simulated traditional CFB I in the following text. To further clarify the effect of the coupled moving bed, as shown in Figure 1c, the whole moving bed was replaced completely with a Plexiglas column connecting the loop seal exit directly to another return point of the riser at a height of about 3.2 m above the gas distributor. Thus, the only difference of this new CFB from the

Table 1. Properties of Fluidizing Particles

d_p (μm)	ρ_s (kg/m^3)	ρ_b (kg/m^3)	U_{mf} (m/s)	U_t (m/s)
378	2600	1470	0.11	2.82

traditional CFB, shown in Figure 1a, is that the effective height of the riser was shortened to about 9.2 m. This lowered CFB will be called as simulated traditional CFB II in this study.

A type of silica sand particles of Geldart B characterized in Table 1 was used as the fluidizing material. The fluidizing medium is compressed air at room temperature. Local pressures at the columns were measured by pressure transducers, and the signals were sampled by a personal computer. Although using a switch valve on the standpipe of a CFB to collect some quantity of recycling particles in a time interval was suggested to be the most accurate method for the measurement of G_s,[7] another standpipe has to be involved for the collection of the particles in this method, which also induces possible difficulty in reintroducing the collected particles into the CFB with continuous operation. A relatively easy and widely adopted method for the measurement of G_s is the use of a butterfly valve fixed at the standpipe, as shown in Figures 1b,c. However, in this study, to ensure the accuracy of the measurement from the butterfly valve, a calibration program was conducted in advance by taking the measurement results from the switch valve as references. The loop seal aeration gas velocity U_{gd} in the downflow side of the seal valve was kept at zero in all experimental runs, because the amount of the loop seal fluidizing air (U_{gu}) leaking into the standpipe was large enough to maintain the particles flowing from the downflow side to the upflow side of the seal valve.

Using a kind of silica sand similar to that characterized in Table 1, IHI (Japan) conducted the measurement of G_s in a CFB configured with traditional structure.[8] Figure 2 shows that the experimental data from IHI agree well with the prediction of the equation of Bi and Fan.[9] The measured G_s increases with increasing superficial gas velocity, U_{gp}, in the riser, but at $U_{gp} = 10$ m/s, the G_s realized in this traditional CFB is only about 100 kg/(m^2·s). This phenomenon, on one hand, indicates that the equation of Bi and Fan[9] is a powerful predictor for the saturation carrying capacity.[7] On the other hand, it is also implied that a high solids flux may be difficult to realize in the traditional CFBs.

The experimental data from the two simulated traditional CFBs in this study further consolidate the aforementioned deduction. As shown in Figure 2, although the bottom bed diameter of 120 mm and the riser height of 12.4 m in the simulated traditional CFB I differ from the standpipe diameter of 80 mm and the effective riser height of 9.2 m in the simulated traditional CFB II, respectively, at the same solids inventory $I_m = 130$ kg, the solids circulation rates measured in the two simulated traditional CFBs agree well with each other, showing that these two factors have little effect on the G_s at the same solids inventory in this study. At a given U_{gp}, even if both the simulated traditional CFBs were operated in a state beyond the point of the saturation carrying capacity, the maximal G_s realizable in the two CFBs is still not more than about 240 kg/(m^2 s). However, in the newly configured CFB, the achievable G_s at the specified U_{gp} is much greater than those in the two simulated traditional CFBs. The G_s realized at the U_{gp} of about 9.6 m/s in the newly configured CFB is as high as around 370 kg/(m^2·s), indicating that the newly configured CFB was truly operated in a high solids flux mode. Because at the fixed solids inventory, the variations of both the returning loop diameter and the effective riser height within the tested range were found to have less effect on the G_s in the riser, the increased G_s in the newly configured CFB when compared with those in both the two simulated traditional CFBs can only be attributed to the coupling of the moving bed in the bottom section of the riser.

In fact, the G_s realizable in the riser of a CFB is most closely influenced only by the pressure head from the standpipe rather than the standpipe height.[10] Because the standpipe top in the three different CFBs was connected into an induced fan, the local pressure was kept nearly constant in this study. So, the local pressure P_{bottom} at the bottom of the returning loop, as shown in Figures 1b,c, can be taken as a fair index to the feed driving force of the returning loop in the three-bed configurations. The higher the local pressure P_{bottom}, the greater is the feed driving force. The experimental data, exemplified in Figure 3, show that all solids circulation rates measured in the three-bed configurations are subject to a similar correlation with the P_{bottom} and the G_s increases proportionally with increasing P_{bottom}, demonstrating that the G_s is surely determined by the feed pressure head of the returning loop in the CFBs.

Compared with the two simulated traditional CFBs, the newly configured CFB provides the maximal pressure head from the returning loop under the same operating conditions, as shown in Figure 3. This is because, on one hand, the moving bed in the newly configured CFB enables the generation of greater pressure head than the standpipe of the same size in the two simulated traditional CFBs. On the other hand, as shown in Figure 4, the throat-type configuration gives rise to an extra flow resistance ΔP_{throat}, but the

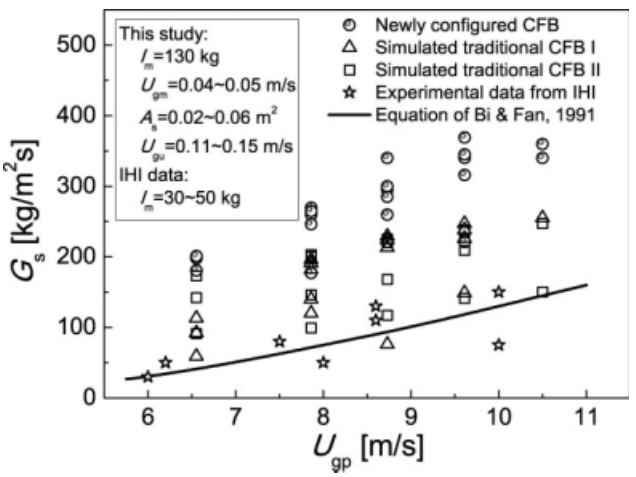

Figure 2. Variation of solids circulation rate, G_s, with superficial gas velocity, U_{gp}.

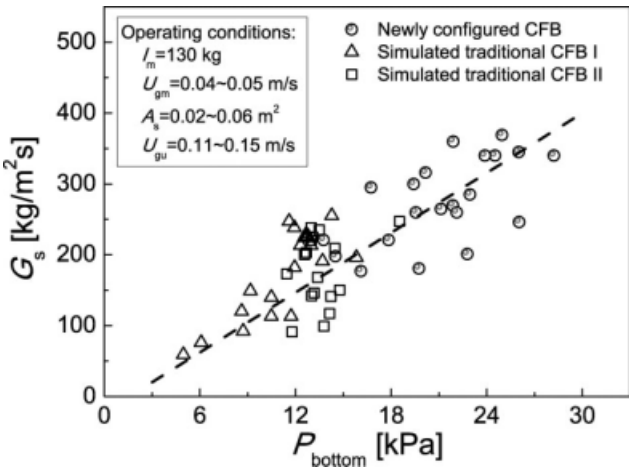

Figure 3. Correlation between solids circulation rate, G_s, and local pressure, P_{bottom}, at the bottom of the returning loop.

resultant resistance of lower than about 2.5 kPa for the tested range of G_s is almost negligible when compared with the flow resistance ΔP_{loop} of around 5.0–18.0 kPa from the loop seal. Leveling up the loop seal above the moving bed in the newly configured CFB does not avoid or decrease the flow resistance from the loop seal, but makes it possible to almost completely convert the raised pressure head from the moving bed into the effective feed driving force by replacing the loop seal with the low-flow-resistance throat-type configuration. Therefore, as shown in Figure 3, about a twice increase of the P_{bottom} in the newly configured CFB correspondingly raises the G_s up to around twice that achievable in the two simulated traditional CFBs under similar operating conditions. This reveals the necessity and feasibility of integrating the moving bed into the bottom section of the riser to realize the desired high solids flux concurrent conveying flow.

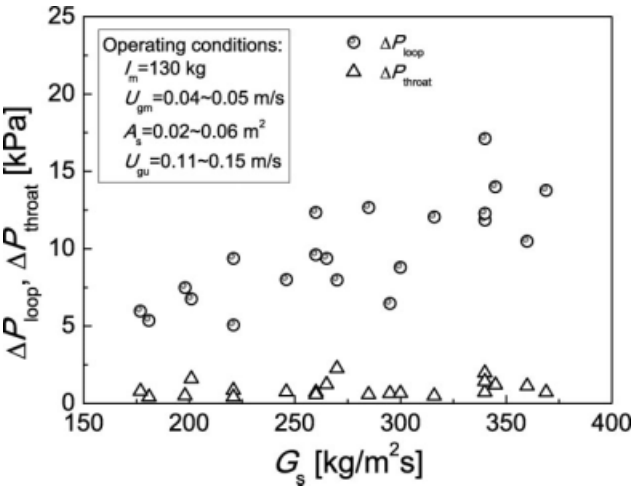

Figure 4. Comparison between the flow resistances (ΔP_{loop} and ΔP_{throat}) from the loop seal and the throat-type configuration in the newly configured CFB.

Conclusions

Coupling a moving bed with a throat-type exit at the riser bottom and elevating the loop seal to above the moving bed in a CFB is feasible to increase the feed driving force of the returning loop and thus to realize high solids flux concurrent conveying flow inside the riser. For the silica sand particles of 378 μm in Sauter mean diameter, solids circulation rates of up to 370 kg/(m^2·s) in the riser are readily achieved at superficial gas velocities of about 9.6 m/s in the new CFB reconfigured according to the proposed idea.

Acknowledgments

The Chinese authors are grateful for the financial support from the National 863 Project under the number 2006AA05A103 and the NSFC Projects under the numbers 20606034 and 20776144. The authors are grateful to Professor Xiaotao Bi for his valuable discussions.

Notation

A_s = cross-sectional area of bottom opening of the loop seal, m^2
d_p = particle diameter, μm
G_s = solids circulation rate, kg/(m^2·s)
I_m = solids inventory, kg
P_{bottom} = pressure at the bottom of the returning loop, kPa
U_{gd} = aeration gas velocity in the downflow side of the loop seal, m/s
U_{gm} = moving bed aeration gas velocity, m/s
U_{gp} = superficial gas velocity in the riser, m/s
U_{gu} = fluidizing gas velocity in the upflow side of the loop seal, m/s
U_{mf} = minimum fluidization velocity of silica sand particles, m/s
U_t = terminal velocity of silica sand particles, m/s
ΔP_I, ΔP_{II} = pressure drop across the column, kPa
ΔP_{loop} = pressure drop across the loop seal, kPa
ΔP_m = pressure drop across the moving bed, kPa
ΔP_{new} = maxima pressure drop across the returning loop of the newly configured CFB, kPa
$\Delta P_{s,new}$ = pressure drop across the standpipe of the newly configured CFB, kPa
$\Delta P_{s,tra}$ = pressure drop across the standpipe of the traditional CFB, kPa
ΔP_{throat} = pressure drop across the throat-type exit of the moving bed, kPa
ΔP_{tra} = maxima pressure drop across the returning loop of the traditional CFB, kPa
ρ_b = bulk density of silica sand, kg/m^3
ρ_s = real density of silica sand, kg/m^3

Literature Cited

1. Corella J, Toledo JM, Molina G. A review on dual fluidized-bed biomass gasifiers. *Ind Eng Chem Res*. 2007;46:6831–6839.
2. Paisley M. A catalytic hot gas conditioning of biomass derived product gas. In: Bridgwater AV, Boocock DGB, editors. *Developments in Thermochemical Biomass Conversion*, Vol. 2. London: Blackie Academic and Professional, 1997:1209–1223.
3. Bi HT, Zhu J. Static instability analysis of circulating fluidized beds and concept of high-density risers. *AIChE J*. 1993;39:1272–1280.

4. Pugsley TS, Milne BJ, Berruti F. An innovative non-mechanical solids feeder for high solids mass fluxes in circulating fluidized bed risers. *Powder Technol*. 1996;88:123–131.
5. Li ZQ, Wu CN, Wei F, Jin Y. Experimental study of high-density gas–solids flow in a new coupled circulating fluidized bed. *Powder Technol*. 2004;139:214–220.
6. Zhu JX, Bi HT. Distinctions between low density and high density circulating fluidized beds. *Can J Chem Eng*. 1995;743:644–649.
7. Xu GW, Murakami T, Suda T, Matsuzawa Y, Tani H. Particle circulation rate in high-temperature CFB: measurement and temperature influence. *AIChE J*. 2006;52:3626–3630.
8. Suda T, Takafugi M, Xu GW. Research on the optimum condition to obtain maximal solid flow rate of CFB, IHI-IPE Joint Workshop, Isogo-Ku, Yokohama, February, 2008.
9. Bi HT, Fan LS. Regime transition in gas–solid circulating fluidized beds, Paper 101e. In Preprint Proceedings of the AIChE Annual Meeting, Los Angeles, CA, 1991.
10. Davis BM, Vimalchand P, Liu GH, Smit PV, Longanbach HJ. Operation of the PSDF transport gasifier, Paper 50–2. In Preprint Proceedings of the Nineteenth Annual Pittsburgh Coal Conference, Pittsburgh, PA, 2002.

Manuscript received Oct. 25, 2008, and revision received Dec. 8, 2008.